Probabilistic Methodology to Estimate Environmental Conditions for Localized Corrosion and Stress Corrosion Cracking of Alloy 22 in a High-Level Radioactive Waste Repository Setting

Osvaldo Pensado and Roberto Pabalan
Center for Nuclear Waste Regulatory Analyses (CNWRA), San Antonio, TX, USA

Abstract

The U.S. Department of Energy (DOE) has indicated that it may use Alloy 22 (Ni-22Cr-13Mo-4Fe-3W) as the waste package outer container material for the potential high-level waste repository at Yucca Mountain, Nevada. This alloy could be susceptible to localized corrosion, in the form of crevice corrosion, and stress corrosion cracking if environmental conditions and material requirements (e.g., existence of crevices or high enough tensile stresses) are met. An approach is proposed to assess the likelihood of environmental conditions capable of inducing crevice corrosion or stress corrosion cracking in Alloy 22. The approach is based on thermodynamic simulations of evaporation of porewaters and published equations to compute corrosion potential and critical potentials for crevice corrosion and stress corrosion cracking as functions of pH, ionic concentration, temperature, and metallurgical states from fabrication processes. Examples are presented to show how the approach can be used in system-level assessment of repository performance.

1. Introduction

The U.S. Department of Energy (DOE) has indicated that for the potential high-level waste repository at Yucca Mountain, Nevada, the waste package may consist of an outer container made of Alloy 22 for corrosion resistance and an inner container made of Type 316 nuclear grade stainless steel for structural support [1]. The waste package is proposed to be protected against seepage water and rockfall arising from gradual degradation of drifts by an independent titanium alloy structure referred to as "drip shield" [1]. Radioactive decay can cause waste packages to experience transient temperatures well above the boiling point of pure water for several hundreds to few thousands of years. Deliquescent multicomponent salt systems have been reported that can form liquid solutions at temperatures as high as 200 °C [392 °F] or above [2]. In principle, those solutions can support electrochemical corrosion processes. Feasible rates of corrosion of Alloy 22 at those elevated temperatures are currently being investigated by other authors. Localized corrosion, in the form of crevice corrosion (CC), and stress corrosion cracking (SCC) of Alloy 22 have been observed in tests conducted in aqueous solutions at temperatures lower than 110 °C [230 °F] [3, 4]. Appropriate environmental conditions (water compositions and temperature) must be established for the initiation and propagation of CC or SCC. If those conditions are not established, Alloy 22 is expected to undergo passive dissolution at corrosion rates of less than 100 nm/yr [0.004 mpy] [1, 3].

The environmental requirements for CC and SCC have been delineated elsewhere [3−12]. Crevice corrosion of Alloy 22 is feasible if (i) tight crevices form, (ii) concentrated chloride solutions are available with low concentrations of oxianions (nitrate, carbonate/bicarbonate, sulfate) capable of inhibiting CC, and (iii) high enough corrosion potentials are attained [3,5−8]. Stress corrosion cracking of Alloy 22 has been observed in bicarbonate solutions containing sufficient concentration of chloride ions at

temperatures above 60 °C [140 °F] using slow strain rate tests with tensile samples polarized at high anodic potentials [9–12]. Therefore, SCC of Alloy 22 appears feasible if (i) the material is affected by high tensile stresses, (ii) solutions are available with enough concentrations of chloride and bicarbonate, and (iii) high enough corrosion potentials are attained [9–12].

The concentrated solutions required for both CC and SCC could form on the waste package by evaporation of seepage water. If seepage does not contact the waste package surface, another source for the formation of aqueous solutions is moisture in the environment. Analyses of dusts gathered in the Yucca Mountain region reveal that sulfate and nitrate are dominant salt components [13–15]. Solutions arising from deliquescence of salts in dust or by mixing of salts with condensed water are envisioned to contain high nitrate concentration to inhibit Alloy 22 crevice corrosion [2,14]. It is recognized, however, that the question of whether deliquescent solutions can support localized corrosion of Alloy 22 is still under investigation. This paper focuses on the scenario where seepage water contacts the waste package. An approach is proposed to assess the likelihood of environmental conditions capable of supporting initiation and propagation of CC or SCC in Alloy 22 under the "waste package seepage contact" scenario. The approach accounts for variability in solution composition, temperature dependencies, and for the different susceptibilities of mill-annealed and weld zones to CC. The methodology is proposed to be used in system-level assessment of repository performance. Qualitative assessment of additional requirements for CC and SCC, such as formation of crevices or development of regions of sufficiently high tensile (residual or applied) stresses, are provided to more thoroughly complement performance assessments.

2. Mathematical approach

2.1 Corrosion potential and critical potentials

The approach for classifying solution compositions as capable of supporting (i.e, initiating and propagating) CC or SCC is based on comparison of the corrosion potential, E_{corr}, to a critical potential, E_{crit}. Thus, for a particular solution composition, if the corrosion potential, E_{corr}, exceeds a critical potential, E_{crit}, the solution is considered capable of promoting a detrimental corrosion mode (CC or SCC).

The critical potential for CC is defined in this paper as the crevice corrosion repassivation potential, E_{rcrev}. It is assumed that, in the long term, E_{rcrev} is the lowest potential at which active crevice corrosion can be initiated and propagated [16]. E_{rcrev} is a function of the temperature, solution composition, and fabrication states (e.g., welded and mill-annealed Alloy 22) [3, 6]. The repassivation potential decreases with increasing chloride concentration and significantly increases if oxyanions such as nitrate, bicarbonate, and sulfate are present in the solution [8]. Empirical relationships for mill-annealed and thermally aged material defining E_{rcrev} as a function of temperature, chloride concentration, and oxyanion concentrations have been published by Dunn et al. [6]. The E_{rcrev} of the thermally aged material defines a lower bound to E_{rcrev} measured in welded samples [6]. Anderko et al. [17] developed a model to compute the repassivation potential of alloys in multicomponent electrolyte systems, accounting for aggressive species such as chloride and inhibiting species such as nitrate. The model accurately predicted the repassivation potential in a number of Fe-Ni-Cr-Mo alloys. The equations by Dunn et al. [6] are consistent with the Anderko et al. expressions. For the

current analysis, the published parameters of the Dunn et al. equations were modified to account for an uncertainty interval in E_{rcrev} spanning 100 mV for thermally aged material and 300 mV for mill-annealed material (the parameters to compute E_{rcrev} according to Dunn et al. [6] correspond to median values in the present analysis). The 300 mV uncertainty interval was derived via confidence bounds in curve-fitting parameters. The values of E_{rcrev} for thermally aged material in general represent a lower bound for the weld material E_{rcrev}. For this reason, a narrower uncertainty envelope, 100 mV wide, was considered for thermally aged material. The uncertainty intervals are assumed constant (i.e., independent of temperature and solution compositions).

To study SCC, Chiang et al. [4, 9, 10, 12] conducted slow strain rate tests selectively removing constituent anionic species (e.g., nitrate, sulfate, fluoride, or chloride) from a solution known to induce SCC to isolate the main ions causing SCC. A synergistic effect was discovered between bicarbonate and chloride ions in SCC of Alloy 22. At a constant bicarbonate level, the susceptibility of Alloy 22 to SCC increases with increasing chloride ion concentration. In pure bicarbonate or chloride solutions, no SCC was observed [4, 9, 10, 12]. At fixed chloride and bicarbonate concentrations, SCC was only observed in alloy samples at high anodic polarization potentials. A critical potential, E_{SCC}, was inferred from the experimental database by analyzing the lowest anodic polarization potentials required to observe the occurrence of SCC [3, 11]. As a first approximation, Shukla et al. [11, 3] proposed a linear equation to compute E_{SCC} as a function of the temperature. In this paper, it is assumed that SCC in Alloy 22 is feasible if the corrosion potential, E_{corr}, exceeds E_{SCC} as defined by Shukla et al. [11, 3].

Based on electrochemical kinetics laws, solving for the potential at which the anodic and cathodic current densities are equal, the following expression for the corrosion potential was derived [3]:

$$E_{corr} = \frac{E_a^a - E_a^{ef}}{Z_r \, \beta_r^{ef} \, F} - \frac{E_a^a}{Z_r \, \beta_r^{ef} \, F} \frac{T}{T_{ref}^a} + \frac{RT}{Z_r \, \beta_r^{ef} \, F} \ln\left[\left(\frac{[H^+]}{\text{mol/L}} \right)^{n_H} \left(\frac{pO_2}{\text{atm}} \right)^{n_O} \frac{i_r^{ef}}{i_a^o} \frac{C_{O_2}^{bulk}(T)}{C_{O_2}^{bulk}(T_{ref})} \right]$$

$$(1)$$

where F is the Faraday constant (9.64867×10^4 C/mol); pO_2, the oxygen partial pressure (0.21 atm); R, the ideal gas constant [8.314 J/(mol K)]; T, the absolute temperature; and $[H^+]$, the concentration of hydrogen ions $\{[H^+] = -\log_{10}(\text{pH})\}$. $C_{O_2}^{bulk}(T)$ is the oxygen concentration in the bulk solution as a function of temperature, and T_{ref} is a reference temperature (298.15 K). $C_{O_2}^{bulk}(T)$ is estimated using the empirical relationship for a pure water system [18]:

$$C_{O_2}^{bulk}(T) = pO_2 \, e^{0.2984 - \frac{5596.17\,\text{K}}{T} + \frac{1.04967 \times 10^6 \,\text{K}^2}{T^2}} \quad \frac{\text{mol}}{\text{kg atm}} \qquad (2)$$

Other variable definitions and values are provided in Table 1. Parameters for Eq. (1) were selected to properly reflect experimental trends of Alloy 22 in a range of temperatures up to 95 °C [203 °F] in full immersion tests. Minimal or no dependencies have been observed between the corrosion potential and the concentration of solutes such as chloride [3]. However, weak dependencies are expected to arise due to oxygen

3

salting out (i.e., reduced concentrations of dissolved oxygen in concentrated solutions). Eq. (1) can be modified to account for salting out effects provided there is an available database of the variation of the corrosion potential as a function of the dissolved oxygen concentration at fixed temperatures. As a first approximation, such a likely dependence is ignored in this paper.

Experimentally, high values of E_{corr} have been observed when the pH falls below 6 (Figure 1) [3]. The transition is due to different kinetics of the cathodic reaction. At high pH, the dominant cathodic reaction is $O_2 + H_2O + 4e^- \rightarrow 4OH^-$, while at low pH, $O_2 + 4H^+ + 4e^- \rightarrow 2H_2O$. Both cathodic reactions lead to an E_{corr} expression of identical form [Eq. (1)] but with different kinetic parameters. For the sake of mathematical simplicity, a sharp transition in E_{corr} is assumed to take place at pH = 6, although experimentally a more gradual transition is expected. The parameter values to compute E_{corr} for the acidic (pH<6) and alkaline range (pH>6) are shown in Table 1.

Insert Figure 1

Figure 1 shows a comparison of Eq. (1) to experimental values by Dunn et al. [3]. Uncertainty in E_{corr} is assumed to be due to the uncertainty in the anodic current density, i_a^o, associated with the passive dissolution of Alloy 22. The anodic current density is defined via a probability density function (Table 1). The resulting bounds in E_{corr} arising from the consideration of uncertainty in i_a^o is shown in Figure 1. The i_a^o probability density function was selected so that the median E_{corr} is symmetrically located between upper and low bounds (Figure 1).

2.2 Solution compositions

There are three potential sources of water to enable corrosion processes —seepage into the drifts from overlying rocks, condensation due to in-drift cold trap processes, and deliquescence of the salts present in dusts deposited on the waste package surface [19, 3]. Salts in dusts could deliquesce and form brines that could support electrochemical corrosion processes at temperatures well beyond the boiling point of pure water. The problem of elevated temperature corrosion is not analyzed in this paper. Solutions formed by dust and condensate mixtures are considered unlikely to promote CC because sulfate and nitrate are dominant salt components of dusts gathered in the Yucca Mountain region [2, 14, 20, 21] and effective localized corrosion inhibitors [8, 3]. In this paper, the scenario of interest is one where drip shields may breach due to rock loads, arising from drift degradation, and deflect inducing localized tensile stresses on the waste package. Under such a scenario, the drip shield could allow contact of seepage water with the waste package. Therefore, the dominant source of water for the SCC scenario of interest is also seepage, as opposed to condensation. The initial composition of seepage will evolve over time as a result of evaporation, and concentrated solutions may form that could support the initiation and propagation of CC and SCC. Therefore, this paper focuses on the analysis of solutions formed by evaporation of seepage waters. The analysis is limited to waste package temperatures up to 110 °C [230 °F]. At rock temperatures above the boiling temperature, deep percolating water may be diverted away due to the vaporization barrier, making the formation of seepage in the drifts difficult. It is considered feasible that percolating water in below-boiling zones in the rock away from drifts could move along fractures intercepting the drifts (fractures in the dryout zone between the boiling isotherm and drift wall) and form seepage, even at drift wall temperatures above boiling [22–24]. These rock wall temperatures control the range of waste package temperatures for the "waste

4

package seepage contact" scenario. It may be unlikely that such waste package temperatures extend far beyond the maximum temperature of 110 °C [230 °F] considered in this paper, but it is recognized that precise threshold temperatures are uncertain.

The approach to estimate distributions of water compositions is described as follows. The composition of seepage is assumed similar to the measured composition of waters in pores of unsaturated zone rock. Thermodynamic simulations of the chemical evolution of in-drift waters resulting from evaporation of porewaters were conducted. The evaporation simulations were conducted using StreamAnalyzer Version 2.0 [25]. The code allows for simulation of aqueous chemical systems for temperatures up to 300 °C [573 °F], pressures up to 1,500 bar [21,800 psi], and ionic strengths up to 30 molal. The evaporation simulations were done at 50, 70, 90, and 110 °C [122, 158, 194, and 230 °F]. The final water vapor pressure was selected as a fraction of the saturation water vapor pressure, with a fraction defined as a function of the waste package temperature (Figure 2, median value). The range and median value in the water vapor saturation fraction (also referred to as *relative humidity*) as functions of the waste package temperature in Figure 2 were determined from data from a performance assessment code executed in Monte Carlo mode to account for uncertainty in thermohydrological rock features. This code was used to compute the waste package temperature and relative humidity of air close to the waste package as functions of time, and from these data the median and bounds in Figure 2 were derived. Uncertainty in the relative humidity at the waste package surface is the result of spatial variability and uncertainty in thermohydrological rock features [26, 27].

Insert Figure 2

The simulations allowed determination of types of brines that may form in emplacement drifts and concentration ranges of these brines. The thermodynamic calculations were supplemented by an alternative approach based on the concept of chemical divide developed by Hardie and Eugster [28]. In the chemical divide concept, the chemical types of brines and salt minerals that form upon evaporation of natural waters are determined by early precipitation of insoluble minerals (e.g., calcite and gypsum). Natural waters at Yucca Mountain are considered to evolve into three types of brines upon evaporation: (i) calcium-chloride, (ii) neutral, and (iii) alkaline [3]. Thirty-three porewater compositions were used as input to the evaporation simulations selected to represent the broad composition range of the more than 150 samples of Yucca Mountain unsaturated zone porewater reported by Yang et al. [29–31]. To provide a basis for estimating the frequency of occurrence of the three brine types and their respective chemical characteristics, the full set of Yang et al. [29–31] data on unsaturated zone porewater compositions was used jointly with the chemical divide concept of Hardie and Eugster [28]. From 156 compositions, 8, 24, and 68 percent resulted into calcium chloride, neutral, and alkaline type brines, respectively. For each of the considered temperatures, distribution functions for pH, [Cl^-], [NO_3^-], [HCO_3^-] + [CO_3^{2-}], and [SO_4^{2-}] were numerically derived by combining the three brine types into a single set, preserving the brine type frequency. The resulting distribution functions were mapped into standard normal distributions (zero mean and unit standard deviation), and correlation matrices of the standardized data were computed. The computed correlation matrices (with entries rounded to one significant digit) are shown in Table 2. As expected, at all analyzed temperatures, there is a positive correlation between pH and the total carbonate concentration ([HCO_3^-] + [CO_3^{2-}]). In general, the chloride concentration, [Cl^-], is negatively correlated to the oxyanion concentrations, [NO_3^-], [HCO_3^-] + [CO_3^{2-}], and [SO_4^{2-}], due to salting out. The magnitude of the correlation

coefficient between [Cl⁻] and [NO₃⁻] increases with increasing temperature. Based on this observation alone, Alloy 22 susceptibility to crevice corrosion, as a function of solution compositions, is higher at higher temperatures. Nonnegligible negative correlations between pH and [Cl⁻] are noted at the lower temperatures (i.e., at lower temperatures, chloride concentrated solutions are also solutions with low pH).

The numerical cumulative distribution functions (CDF) for pH and the concentration of the various anionic species are shown in Figure 3 for the various temperatures considered. The pH range tends to increase as the temperature decreases, with a more pronounced temperature dependence on the low end of the pH distribution (Figure 3-A). The low bound of the chloride concentration distribution tends to decrease as a function of increasing temperature. Most likely, this behavior is the result of salting out (e.g., as the concentration of other solutes such as nitrate increases with increasing temperature, the chloride solubility decreases). Conversely, the upper range of the chloride concentration distribution is an increasing function of the temperature (Figure 3-B). The broader nitrate concentration ranges as a function of increasing temperature are a result of enhanced solubility at higher temperatures (Figure 3-C). The total carbonate, [HCO_3^-] + [CO_3^{2-}], on the other hand, exhibits retrograde solubility, with higher concentrations at lower temperatures (Figure 3-D). The sulfate ion, [SO_4^{2-}], also approximately exhibits some retrograde solubility (higher concentrations are in general associated with the lower temperatures, as in Figure 3-E).

The distribution functions in Figure 3 and the correlation matrices (of standardized data) in Table 2 summarize end compositions after evaporation at various temperatures. To allow for more complete consideration of water composition uncertainty/variability, *feasible* water compositions were constructed by stochastic sampling of the distribution functions in Figure 3, preserving the correlation matrices in Table 2. A water composition is a vector of the form {pH, [Cl⁻], [NO_3^-], [HCO_3^-] + [CO_3^{2-}], [SO_4^{2-}]}. A *feasible* sample of water compositions is a set of vectors such that the numerical cumulative distribution of each vector entry (e.g., pH) is consistent with the distributions in Figure 3, and the correlation matrix of the standardized set of vectors is consistent with Table 2. By adopting such a stochastic sampling approach, a broader set of water compositions than those arising from the thermodynamic simulations can be considered.

Insert Figure 3

2.3. Sampling approach

For each temperature analyzed, a stochastic sample of 10,000 feasible water compositions were numerically generated by following the algorithm described by Helton and Davis to construct correlated samples based on the Cholesky factorization of a covariance matrix [32]. This algorithm justifies the adoption of standardized correlation matrices, as the Cholesky-factorization algorithm accurately reproduces predefined correlation matrices. For any water composition in the stochastic sample, E_{corr} was computed as a function of pH, the waste package temperature, and the anodic current density (which was sampled from the triangular distribution for i_a^o in Table 1). For the CC analysis, the repassivation potential, E_{rcrev}, was computed as a function of the temperature and the ionic concentrations [Cl⁻], [NO_3^-], [HCO_3^-] + [CO_3^{2-}], and [SO_4^{2-}]. Two different values of E_{rcrev} were computed for mill-annealed and thermally aged material (the latter was selected as lower bound for Alloy 22 welds). Uncertainty in E_{rcrev} was incorporated by an additive uncertainty term in the range (−50, 50) mV for mill-annealed material, and in the range (−150, 150) mV for thermally aged material; both

terms were stochastically sampled from symmetric triangular distributions. E_{crit} for SCC, E_{SCC}, was computed as a function of the temperature according to an expression reported in the literature [11, 4]. An uncertainty term was added to E_{SCC} sampled from a symmetric triangular distribution spanning from –50 to 50 mV. The fraction of the number of solution compositions satisfying $E_{corr} > E_{crit}$ is an estimator of the probability of the formation of solution compositions capable of promoting the initiation and propagation of CC or SCC, $P(E_{corr} > E_{crit})$.

3. Results and discussion

3.1 Crevice corrosion analysis

Figure 4 presents scatter plots of $E_{corr} – E_{rcrev}$ for mill-annealed Alloy 22 at 110 °C [230 °F] versus pH and concentrations of the various anionic species. The plots summarize 10,000 water compositions, constructed following the stochastic sampling previously described. The fraction of the number of points above the horizontal axis is an estimator of $P(E_{corr} > E_{crit})$ (all of the scatter plots in Figure 4 include the same number of points above the horizontal axis). In general, the points above the horizontal axis are well spread with respect to pH and the anion concentrations, with the exception of nitrate. In the case of nitrate, $E_{corr} – E_{rcrev} > 0$ only if the nitrate concentration is low. Similar analyses were performed at the other temperatures and for thermally aged material, but the scatter plots are not shown for the sake of brevity. The results are summarized in Figure 5, indicating the probability of formation of solution compositions capable of promoting the CC initiation.

> Insert Figure 4

Figure 5 shows the fraction of points satisfying $E_{corr} – E_{rcrev} > 0$. Thermally aged material has higher susceptibility to crevice corrosion than mill-annealed material. Figure 5 indicates that CC is feasible in a range of temperatures. At 50 °C [122 °F], $P(E_{corr} > E_{rcrev})$ is of the order of 10^{-4} for mill-annealed material, and 0.01 for thermally aged material. At 110 °C [230 °F], $P(E_{corr} > E_{rcrev})$ is of the order of 0.05 for mill-annealed material and 0.13 for thermally aged material. These probabilities are different compared to those derived from similar computations by Pensado et al. [5] at 110 °C [230 °F] (0.03 and 0.26 for mill-annealed and thermally aged material, respectively). The lower value of $P(E_{corr} > E_{rcrev})$ for thermally aged material in the present analysis is due to (i) updated thermodynamic simulations and (ii) consideration of complete saturation of air with water vapor in Reference 5 as opposed to partial saturation in the present analysis. Interestingly, lower water vapor saturation leads to more concentrated systems but with higher nitrate concentrations. The higher nitrate-to-chloride ratio in the present analysis is responsible for the lower value of $P(E_{corr} > E_{rcrev})$ for thermally aged Alloy 22 computed at 110 °C [230 °F] compared to the previous evaluation.

> Insert Figure 5

The calculated values of $P(E_{corr} > E_{rcrev})$ do not necessarily imply that waste packages in the repository setting could exhibit CC. The condition $E_{corr} > E_{rcrev}$ is only one requirement for CC initiation. Additional requirements must be satisfied for CC to occur, leading to breaching of the waste package and potential release of radionuclides. The probability, P_T, for a waste package to release radionuclides can be computed as

$$P_T = P_S \ P_R \ \mathrm{P}(E_{corr} > E_{crit}) P_{WF} \tag{3}$$

7

where P_s is the probability for seepage water to contact a waste package; P_R, the probability of formation of appropriate localized corrosion initiation sites (e.g., crevices) including the availability of concentrated solutions at such sites; and P_{WF}, the probability for water to contact and mobilize the waste form in a waste package breached by crevice corrosion. The term P_s is usually computed in performance assessments as a function of scenarios for drip shield failure (e.g., mechanical collapse, general corrosion, hydrogen-induced cracking, creep). The term P_R has appreciable amounts of uncertainty, depending on the scenario being considered. For example, under a drip shield collapse scenario, crevices could form by contact of the drip shield with the waste package. A concentrated solution must also be available at the crevice site for the initiation of localized corrosion. Recent experimental studies analyzing metal-to-metal crevices indicate a strong dependence of CC initiation on crevice characteristics (e.g., geometry, metal composition) [33]. Crevices could also form on the waste package by contact with the support system in the drifts. The probability P_R should be much smaller for welded regions given that welds may only comprise a small percent of the waste package surface. At this time, a value of P_R has poorly constrained uncertainties, which could be addressed by expert elicitation. It is clear that P_R must be significantly less than one. Focusing on an order of magnitude estimate, a value $P_R \leq 0.1$ appears a reasonable selection based on current information. Finally, the term P_{WF} (probability of water contact and mobilization of waste forms in waste packages breached by CC) could be close to one, given the long timeframes of interest. If the waste package is breached by CC, then water likely would continue to be available at the breached location, which would increase the chance for water to infiltrate the waste package. Also, CC breached sites could open as time elapses, increasing the chance for waste forms to be contacted and mobilized by water. Therefore, a value $P_{WF} = 1$ appears reasonable based on current information.

3.2 Stress corrosion cracking analysis

The SCC analysis was slightly different than the CC analysis. In this case, independent analyses were carried out for each of the brine types. Figure 6 is the cumulative distribution function for the total carbonate in solution, $[HCO_3^-] + [CO_3^{2-}]$, for the three brine types at 110 °C [230 °F]. For SCC to occur, bicarbonate must be present in the solution in sufficient concentration [10, 4]. Chiang el at. [4, 9, 10, 12] noted SCC in solutions with bicarbonate concentrations greater than 0.5 molal. From this information, it is inferred that the minimal concentration of bicarbonate needed for SCC may be a fraction of a molar, but the precise threshold value is uncertain at this time. From Figure 6, assuming 0.001 mol/L as threshold value, there is not enough bicarbonate in the calculated Ca-Cl brines to support SCC. In the neutral brines, the total carbonate in the system exceeds 0.001 mol/L in only a small fraction of the compositions. Only in the calculated alkaline brines there is sufficient concentration of the total carbonate to support SCC in a large proportion of the water compositions. However, as noted in Figure 1, the corrosion potential decreases with increasing pH and high values of the corrosion potential are also needed for the initiation of SCC [10, 4]. This competition between high corrosion potentials (attainable at low pH) and sufficient bicarbonate concentrations (attainable at high pH) make $E_{corr} > E_{SCC}$ unlikely. Following the mathematical sampling approach previously described, it is estimated $P(E_{corr} > E_{SCC}) = 4 \times 10^{-5}$ for neutral brines and $P(E_{corr} > E_{SCC}) = 5 \times 10^{-5}$ for alkaline brines at 110 °C [230 °F], assuming a minimal threshold total carbonate value of 10^{-4} mol/L. Considering the 24 and 68 percent estimated frequency of occurrence for neutral and alkaline brines, respectively, results in a combined average of $P(E_{corr} > E_{SCC}) = 4.8 \times$

Insert Figure 6

10^{-5} at 110 °C [230 °F].

As the temperature decreases, SCC is less likely to occur. To derive a notion on the temperature range where SCC is feasible the equation $\text{Max}(E_{corr}) = \text{Min}(E_{SCC})$ was examined. Because E_{corr} is a function of pH and temperature and E_{SCC} is, as a first approximation, a function of the temperature only (assuming that bicarbonate and chloride ions are available above minimal concentrations), the equation is satisfied for a set of pH and temperature values. The solution of the equation is presented in Figure 7. The set of points {T, pH} satisfying $\text{Max}(E_{corr}) = \text{Min}(E_{SCC})$ is approximately a straight line with positive slope (Figure 7). The collection of points {T, pH} below this line defines a region where E_{corr} might exceed E_{crit}. Above the line, SCC is not feasible as $E_{corr}<E_{crit}$. From the thermodynamic simulations at 70, 90, and 110 °C [158, 194, and 230 °F], the total carbonate concentration of the brines was less than 10^{-4} mol/L for pH< 9, which is insufficient to promote SCC. The region below the line $\text{Max}(E_{corr}) = \text{Min}(E_{SCC})$ and above the line pH = 9 defines the region where SCC is feasible (indicated with solid lines in Figure 7). According to Figure 7, SCC is unlikely at temperatures less than 100 °C [212 °F].

A number of uncertainties must be acknowledged that may limit the generality of the conclusions drawn from the present analysis. First, there is uncertainty in the critical potential for SCC. E_{SCC} was determined using a slow strain rate test (SSRT) performed over two weeks using a strain rate of about 2×10^{-6} s^{-1}. The transition between no SCC to SCC appeared smooth as a function of the applied potential in the slow strain rate tests [10, 9, 4]. Therefore, some degree of judgment was unavoidable in determining a threshold value, E_{SCC}, separating tests where SCC was observed from instances where SCC was not. Another source of uncertainty is the possible dependence of E_{SCC} on the strain rate in SSRT. Given that two-week SSRT experiments can only capture SCC with an induction or initiation time shorter than two weeks, it is possible that use of slower strain rates may yield lower values of E_{SCC}. Additional experiments could reduce uncertainties in reported values of E_{SCC}. A second relevant point is the uncertainty in the existence of other solution compositions and systems that may also promote SCC. Using a combinatorial analysis in complex solutions where SCC was known to occur, two principal solution components in the SCC process were identified: chloride and bicarbonate [10, 9, 4]. However, there is no complete certainty that these are the only ions promoting SCC in Alloy 22. These caveats are provided to exercise caution in the use of the information in Figure 7 and estimated values of $P(E_{corr} > E_{SCC})$.

For abstraction of CC and SCC processes in a performance assessment, an equation equivalent to Eq. (3) can be proposed. The interpretation of the term P_R is slightly different for SCC. It represents the probability of the development of regions of sufficient tensile stress in contact with brines capable of supporting (i.e., initiating and propagating) SCC. Likewise in the CC case, P_R is clearly less than one, but it is highly uncertain and relies on expert judgment. As for the CC case, a value $P_R \le 0.1$ appears reasonable. The fact that $P(E_{corr} > E_{SCC})$ is estimated to be low facilitates simplified computations for a performance assessment. For example, assuming that each waste package could experience an independent water chemistry, the number of waste packages that could be affected by SCC can be computed as a Poisson distribution with a recurrence rate $ = P_R \times P(E_{corr} > E_{SCC})$; i.e.,

$$P_n = \frac{(\lambda N)^n}{n!} e^{-\lambda N} \qquad (4)$$

where P_n is the probability of n waste packages undergoing SCC and N is the total number of waste packages contacted by seepage water. If $N = 10^4$ and $P_R = 1$, the probability for at least one waste package to undergo SCC is 0.38. If $P_R = 0.1$, the probability is only 0.05. If $P_R = 1$, substitution of $n \geq 6$ into equation (4) results in $P_n \leq 10^{-5}$, which means that it would be unlikely for more than six waste packages to be affected by SCC. In other words, if environmental and material conditions exist for the occurrence of SCC in the repository system, very few waste packages would be affected. Again, the probability values are only provided to demonstrate the use of Eq. (4). Some caution should be exercised in using these numbers given the uncertainties previously discussed.

4. Conclusions

An approach was developed to assess the likelihood of environmental conditions capable of supporting (i.e., initiating and propagating) CC or SCC of an Alloy 22 waste package in potential repository aqueous environments. The approach was based on thermodynamic simulations of evaporation of porewaters and published equations to compute corrosion potential, E_{corr}, and critical potentials, E_{crit}, for CC and SCC as functions of pH, ionic concentration, temperature, and waste package fabrication states. From probability distribution functions for solution compositions and correlation matrices derived from thermodynamic simulations, the probability for E_{corr} to exceed E_{crit}, $P(E_{corr} > E_{crit})$, was estimated for both CC and SCC. The probability $P(E_{corr} > E_{rcrev})$ was defined as a function of Alloy 22 metallurgical states from waste package fabrication processes (mill-annealed or thermally aged) in the CC analysis. It was found that $P(E_{corr} > E_{rcrev})$ for CC ranges from a few percent to 13 percent for temperatures ranging from 50 to 110 °C [122 to 230 °F]. To support performance assessments, an approach to estimate the percentage of waste packages breached by CC and contributing to radionuclide release was proposed, that depends on definition of additional conditional probabilities related to the likelihood of the formation of crevices conducive to localized corrosion. With respect to SCC, the analysis suggested that SCC is a process feasible at temperatures above the boiling point of pure water, however unlikely. SCC is unlikely due to competing requirements of sufficient bicarbonate concentrations and high corrosion potentials. Uncertainties in the analysis were acknowledged, that could be addressed with additional experimental studies on SCC. Examples are presented to show how the approach might be used in system-level assessment of repository performance

References

[1]   Bechtel SAIC Company, LLC, Technical Basis Document No. 6: Waste Package and Drip Shield Corrosion, Revision 1, Bechtel SAIC Company, LLC, Las Vegas, Nevada, 2003.

[2]   J.A. Rard, K.J. Staggs, S.D. Day, S.A. Carroll, Boiling Temperature and Reversed Deliquescence Relative Humidity Measurements for Mineral Assemblages in the $NaCl + NaNO_3 + KNO_3 + Ca(NO_3)_2 + H_2O$ System, Journal of Solution Chemistry 35 (2006) 1187-1215.

[3]   D.S. Dunn, O. Pensado, Y.-M. Pan, R.T. Pabalan, L. Yang, X. He, K.T. Chiang, Passive and Localized Corrosion of Alloy 22—Modeling and Experiments, CNWRA 2005-02, San Antonio, Texas, 2005.

[4]   K.T. Chiang, D.S. Dunn, Y.-M. Pan, O. Pensado, P.K. Shukla, Stress Corrosion Cracking of Waste Package Materials—Modeling and Experiments, CNWRA 2007-01, San Antonio, Texas, 2006.

[5]   O. Pensado, R. Pabalan, D. Dunn, K.-T. Chiang, Use of Alloy-22 as a Long-Term Radioactive Waste Containment Material, in: P. Marcus, V. Maurice (Eds.), Passivation of Metals and Semiconductors, and Properties of Thin Oxide Layers — A Selection of Papers from the 9th International Symposium, Paris, France, 27 June – 1 July, 2005, Elsevier, The Netherlands, 2006, pp. 53-57.

[6]   D.S. Dunn, O. Pensado, Y.-M Pan, L.T. Yang, X. He, Modeling Corrosion Processes for Alloy 22 Waste Packages, in: P. Van Isheghem (Ed.), Scientific Basis for Nuclear Waste Management XXIX, Mater. Res. Soc. Symp. Proc. 932, Warrendale, Pennsylvania, 2006, pp. 853-860.

[7]   D.S. Dunn, O. Pensado, G.A. Cragnolino, Performance Assessment of Alloy 22 as a Waste Package Outer Barrier, CORROSION 2005, paper 588, NACE International, Houston, Texas, 2005.

[8]   D.S. Dunn, L. Yang, C. Wu, and G.A. Cragnolino. Effect of Inhibiting Oxyanions on the Localized Corrosion Susceptibility of Waste Package Container Materials, in: J.M. Hanchar, S. Stroes-Gascoyne, L. Browning (Eds.), Scientific Basis for Nuclear Waste Management XXVIII, Mat. Res. Soc. Symp. Proc. 824, Warrendale, Pennsylvania, 2004, pp. 33-38.

[9]   K.T. Chiang, D.S. Dunn, G.A. Cragnolino, Effect of Simulated Groundwater Chemistry on Stress Corrosion Cracking of Alloy 22, CORROSION 2005, paper 05463, NACE International, Houston, Texas, 2005.

[10]   K.T. Chiang, D.S. Dunn, G.A. Cragnolino, The Combined Effect of Bicarbonate and Chloride Ions on the Stress Corrosion Cracking Susceptibility of Alloy 22, CORROSION 2006, paper 06506, NACE International, Houston, Texas, 2006.

[11]   P.K. Shukla, D.S. Dunn, K.T. Chiang, O. Pensado, Stress Corrosion Cracking Model for Alloy 22 in the Potential Yucca Mountain Repository Environment, CORROSION 2006, paper 06502, NACE International, Houston, Texas, 2006.

[12]   K.T. Chiang, D.S. Dunn, and G.A. Cragnolino, Effect of Simulated Groundwater Chemistry on Stress Corrosion Cracking of Alloy 22, Corrosion 63 (2007) 940-950.

[13]   M.C. Reheis, Dust Deposition in Nevada, California, and Utah, 1984-2002, Open-file Report 03-138, U.S. Geological Survey, 2003.

[14]   M.R. Juckett, Deliquescence Relative Humidities of Salts and Natural Dusts Present in the Proposed Underground Repository at Yucca Mountain, Nevada, M.S. Thesis, The University of Texas at San Antonio, San Antonio, Texas, 2006.

[15]   Z.E. Peterman, T.A. Oliver, Geochemistry of Natural Components in the Near-Field Environment, Yucca Mountain, Nevada, in: D.S. Dunn, C. Poinssot, B. Begg,

(Eds.), Materials Research Society Symposium on the Scientific Basis for Nuclear Waste Management XXX, Mat. Res. Soc. Symp. Proc. 985, Warrendale, Pennsylvania, 2007 (in press), paper 0985-NN13-10.

[16] D.S. Dunn, G.A. Cragnolino, N. Sridhar, An Electrochemical Approach to Predicting Long-Term Localized Corrosion of Corrosion-Resistant High-Level Waste Container Materials, Corrosion 56 (2000) 90-104.

[17] A. Anderko, N. Sridhar, D. S. Dunn, A general model for the repassivation potential as a function of multiple aqueous solution species, Corrosion Science 46 (2004) 1583-1612.

[18] R. Batino (Ed.), International Union of Pure and Applied Chemistry (IUPAC) Solubility Data Series: Oxygen and Ozone, Pergamon Press, New York, 1981, p. 7.

[19] L. Browning, R. Fedors, L. Yang, O. Pensado, R. Pabalan, C. Manepally, B. Leslie, Estimated Effects of Temperature-relative Humidity Variations on the Composition of In-Drift Water in the Potential Nuclear Waste Repository at Yucca Mountain, Nevada, in: J.M. Hanchar, S. Stroes-Gascoyne, L. Browning (Eds.), Scientific Basis for Nuclear Waste Management XXVIII, Mat. Res. Soc. Symp. Proc. 824, Warrendale, Pennsylvania, 2004, pp. 417-424.

[20] Z.E. Peterman, J.B. Paces, L.A. Neymark, D. Hudson, Geochemistry of Dust in the Exploratory Studies Facility, Yucca Mountain, Nevada, Proceedings of the 10th International High-Level Radioactive Waste Management Conference, Las Vegas, Nevada, March 30–April 3, 2003 (Published in CD-ROM), American Nuclear Society, La Grange Park, Illinois, 2003.

[21] National Atmospheric Deposition Program (NRSP–3)/National Trends Network, Annual Data Summary for Site: CA95 (Death Valley National Park—Cow Creek). http://nadp.sws.uiuc.edu/nadpdata/ads.asp?site=CA95, Illinois State Water Survey 2000–2003, NADP Program Office, Champaign, Illinois, May 17, 2004.

[22] R.T. Green and J.D. Prikryl, Formation Of A Dry-out Zone Around A Heat Source In A Fractured Porous Medium, in: Proceedings for the Second International Symposium on Two-Phase Flow Modeling and Experimentation, Pisa, Italy, May 23–26, 1999, Edizioni ETS, Italy, 1999.

[23] R.T. Green and J.D. Prikryl, Penetration of the Boiling Isotherm by Flow Down a Fracture, in: Proceedings of the Third International Symposium on Multiphase Flow, Lyon, France, June 8–12, 1998. Technomic Publishing Co., Lyon, France, 1998.

[24] H. Basagaoglu, K. Das, R. Fedors, R. Green, C. Manepally, S. Painter, O. Pensado, S. Stothoff, J. Winterle, and D. Wyrick, Seepage Workshop Report, CNWRA, San Antonio, Texas, 2007.

[25] OLI Systems, Inc., A Guide to Using the OLI Software for version 2.0 of the Analyzers, OLI Systems Inc., Morris Plains, New Jersey, 2005.

[26] R. Fedors, S. Green, D. Walter, G. Adams, D. Farrell, S. Svedeman, Temperature and Relative Humidity Along Heated Drifts With and Without Drift Degradation, CNWRA 2004-04, San Antonio, Texas, 2004.

[27] C. Manepally, R. Fedors, Edge-Cooling Effect on the Potential Thermohydrologic Conditions at Yucca Mountain, Proceedings of the 10th International High-Level Radioactive Waste Management Conference, Las Vegas, Nevada, March 30–April 3, 2003 (Published in CD-ROM), American Nuclear Society, La Grange Park, Illinois, 2003.

[28] L.A. Hardie, H.P. Eugster, Evolution of Closed-basin Brines, Mineralogical Society of America, Special Paper No. 3 (1970) 273-290.

[29] I.C. Yang, Z.E. Peterman, K.M. Scofield, Chemical analyses of pore water from boreholes USW SD-6 and USW WT-24, Yucca Mountain, Nevada, Journal of Contaminant Hydrology 62-63 (2003) 361-380.

[30] I.C. Yang, P. Yu, G.W. Rattray, J.S. Ferarese, J.N. Ryan, U.S. Geological Survey Water-Resources Investigations Report 98-4132, Denver, Colorado, 1998.

[31] I.C. Yang, G.W. Rattray, Y. Pei, U.S. Geological Survey Water-Resources Investigations Report 96-4058, Denver, Colorado, 1996.

[32] J.C. Helton, F.J. Davis, Latin Hypercube Sampling and the Propagation of Uncertainty in Analyses of Complex Systems, Sandia Report SAND2001–0417, Sandia National Laboratories, Albuquerque, New Mexico, and Livermore, California, 2002, pp. 25-27.

[33] X. He, D.S. Dunn, Crevice Corrosion Propagation Behavior of Alloy 22 in Extreme Environments, CORROSION 2007, paper 07578, NACE International, Houston, Texas, 2007.

Table 1: Parameters for the computation of the corrosion potential, E_{corr}, as a function of pH and temperature [2].

Parameter	Definition	Value pH<6	Value pH>6
E_a^a (kJ/mol)	Effective activation energy for the anodic current density	44.7	44.7
E_a^{ef} (kJ/mol)	Effective activation energy for the cathodic current density	40	40
n_H	Dimensionless constant	0.026	0.019
n_O	Dimensionless constant	0.013	0.025
i_a^o (A/cm^2)	Anodic current density at the reference temperature T_{ref}^a	Sampled from a triangular probability distribution function with extremes at 5×10^{-9} and 2×10^{-8}, and with a maximum (mode) at 6.76×10^{-9}.	
i_r^{ef} (A/cm^2)	Reference cathodic current density	0.024	0.017
T_{ref}^a (K)	Reference temperature for the anodic current density	368.15	368.15
Z_r	Number of electrons in the cathodic reaction	4	4
β_r^{ef}	Effective charge transfer coefficient or Taffel constant for the cathodic reaction	0.013	0.025

Table 2: Correlation matrices of standardized data (data mapped to follow a normal distribution with zero mean and unit standard deviation).

|	pH	$[Cl^-]$	$[NO_3^-]$	$[HCO_3^-]$ + $[CO_3^{2-}]$	$[SO_4^{2-}]$
50 °C [122 °F]					
pH	1.0	−0.7	−0.2	0.7	0.3
$[Cl^-]$	−0.7	1.0	-0.3	−0.7	−0.1
$[NO_3^-]$	−0.2	−0.3	1.0	-0.1	−0.4
$[HCO_3^-]$ + $[CO_3^{2-}]$	0.7	−0.7	−0.1	1.0	0.4
$[SO_4^{2-}]$	0.3	−0.1	−0.4	0.4	1.0
70 °C [158 °F]					
pH	1.0	−0.5	−0.2	1.0	0.7
$[Cl^-]$	−0.5	1.0	-0.3	−0.6	−0.4
$[NO_3^-]$	−0.2	−0.3	1.0	−0.1	−0.4
$[HCO_3^-]$ + $[CO_3^{2-}]$	1.0	−0.6	−0.1	1.0	0.7
$[SO_4^{2-}]$	0.7	−0.4	−0.4	0.7	1.0
90 °C [194 °F]					
pH	1.0	0.0	0.0	0.8	0.5
$[Cl^-]$	0.0	1.0	−0.4	−0.1	0.0
$[NO_3^-]$	0.0	−0.4	1.0	0.0	−0.5
$[HCO_3^-]$ + $[CO_3^{2-}]$	0.8	−0.1	0.0	1.0	0.6
$[SO_4^{2-}]$	0.5	0.0	−0.5	0.6	1.0
110 °C [230 °F]					
pH	1.0	−0.2	0.0	0.7	0.2
$[Cl^-]$	−0.2	1.0	−0.5	−0.4	0.2
$[NO_3^-]$	0.0	−0.5	1.0	0.2	−0.8
$[HCO_3^-]$ + $[CO_3^{2-}]$	0.7	−0.4	0.2	1.0	0.1
$[SO_4^{2-}]$	0.2	0.2	−0.8	0.1	1.0
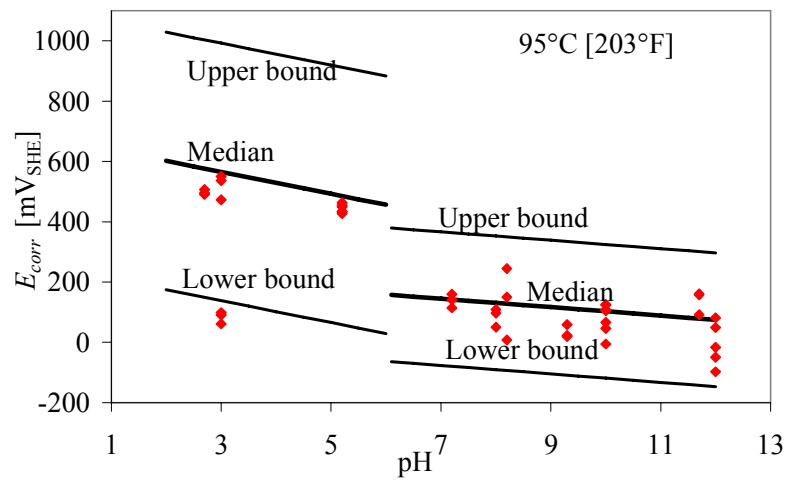
Figure 1
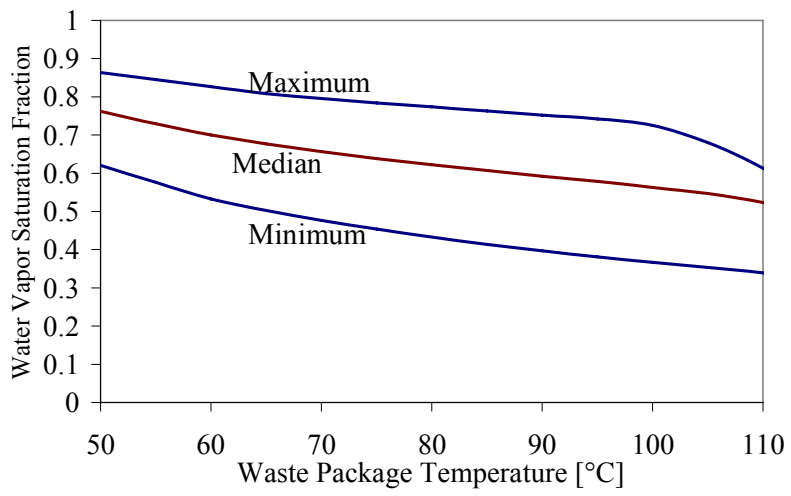
Figure 2
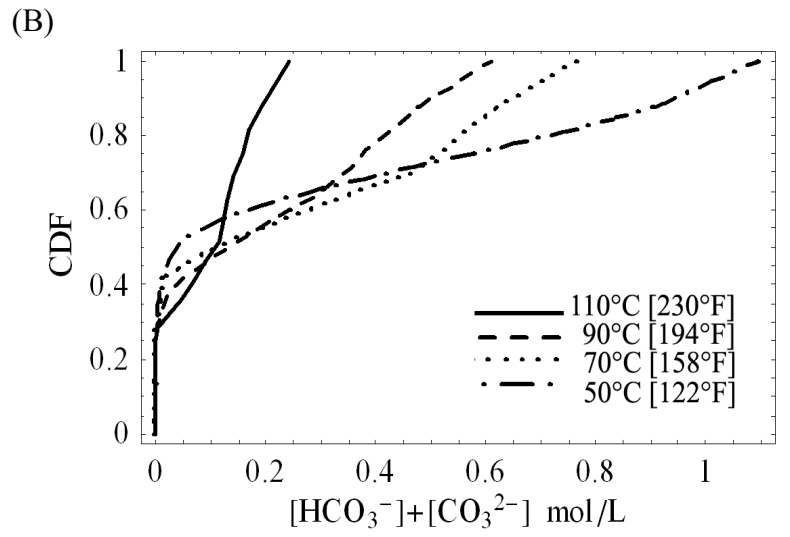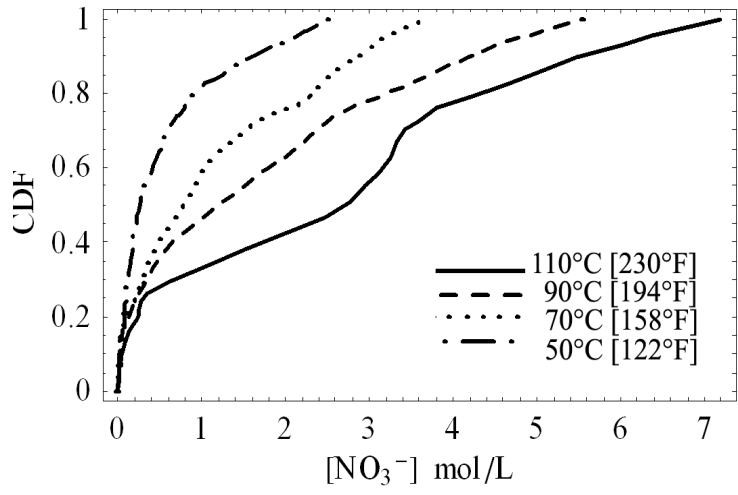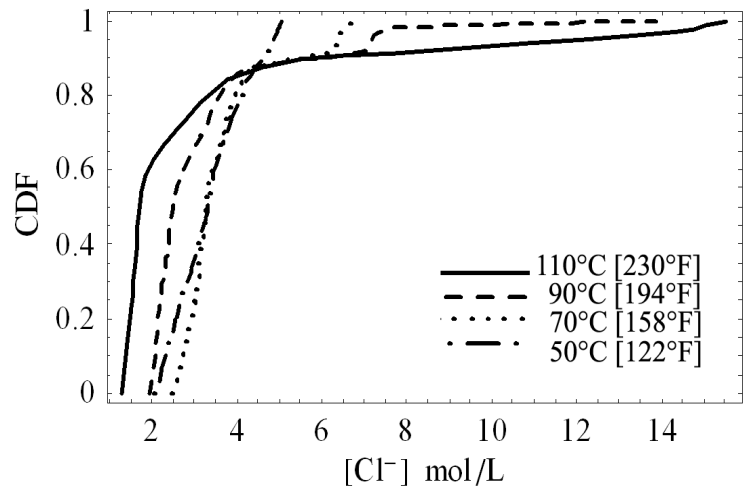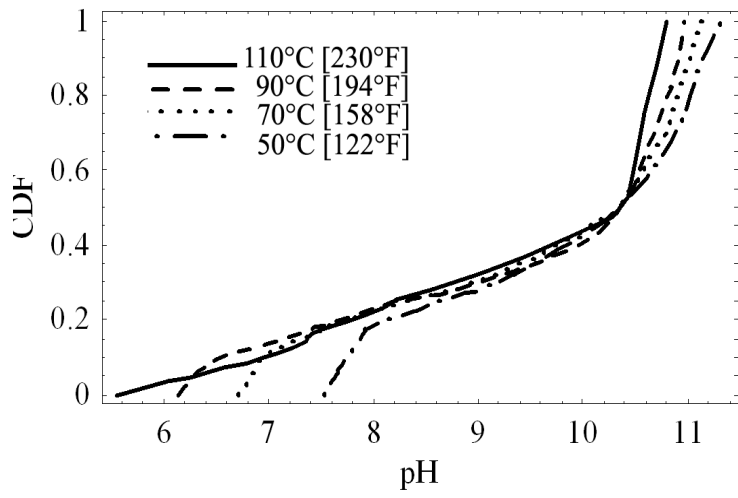
Figure 3
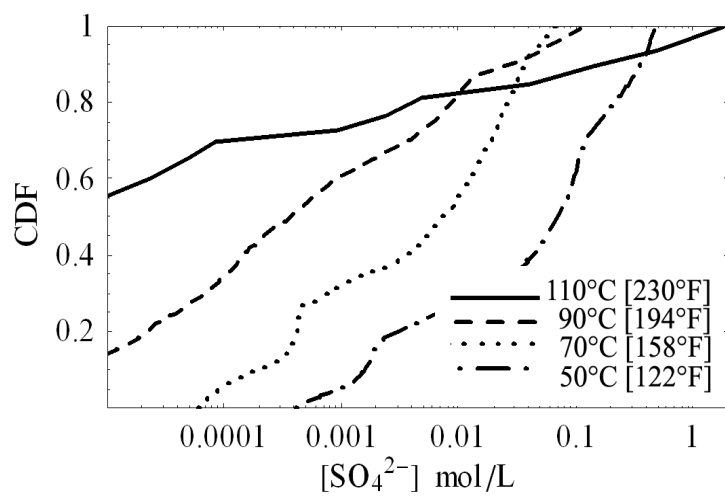
(E)
Figure 3 (Continued)
Figure 3
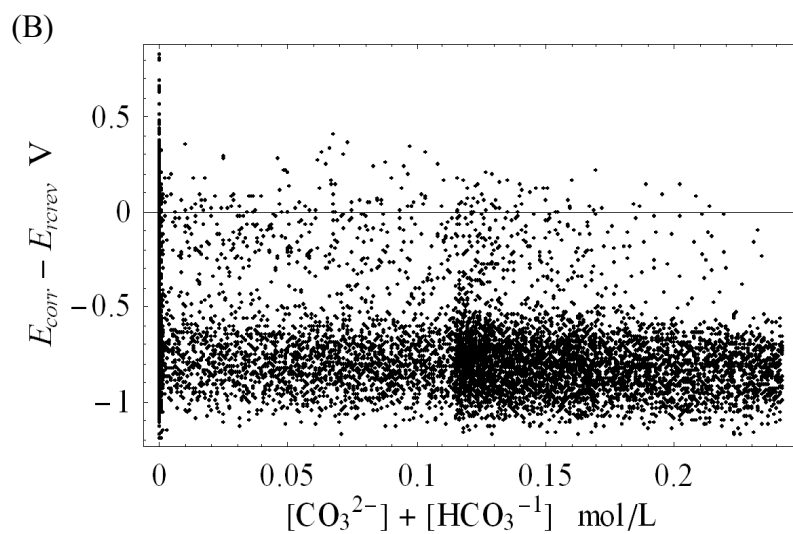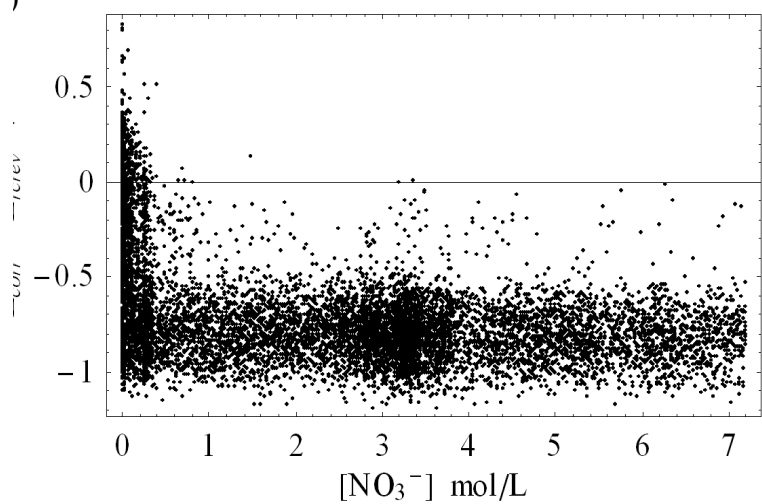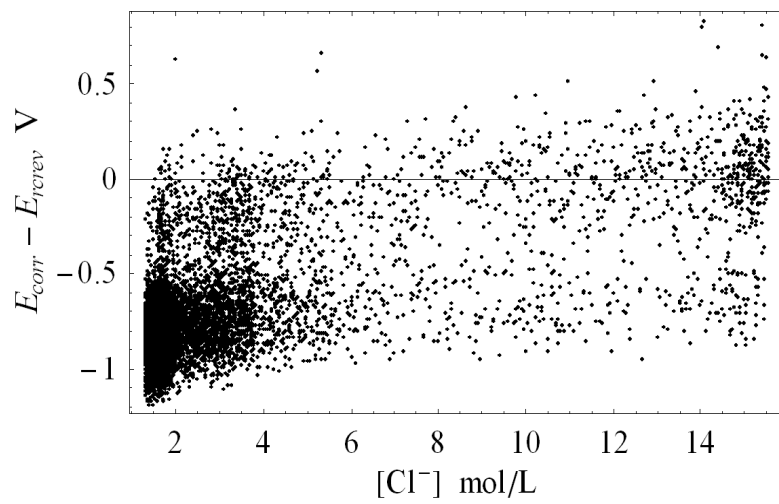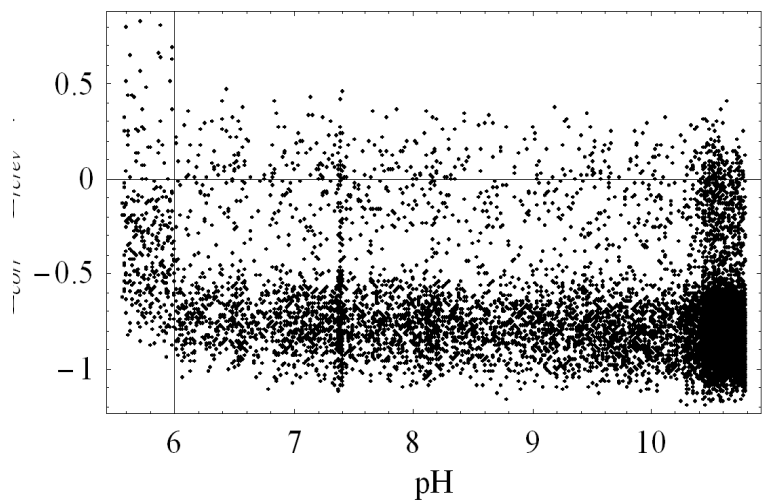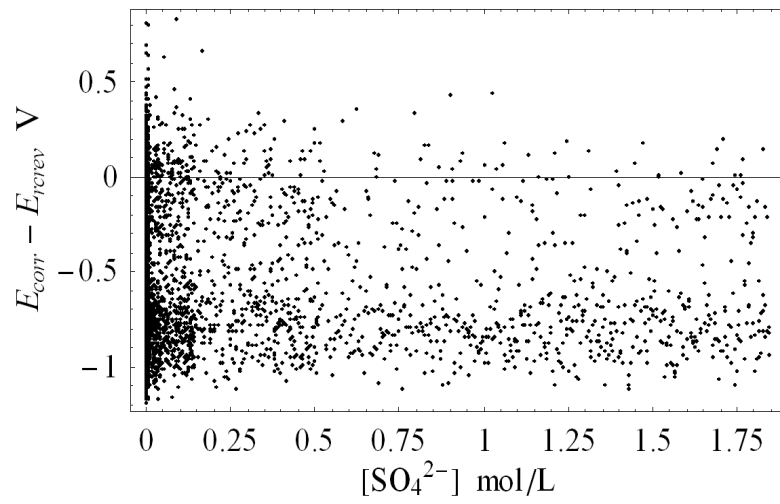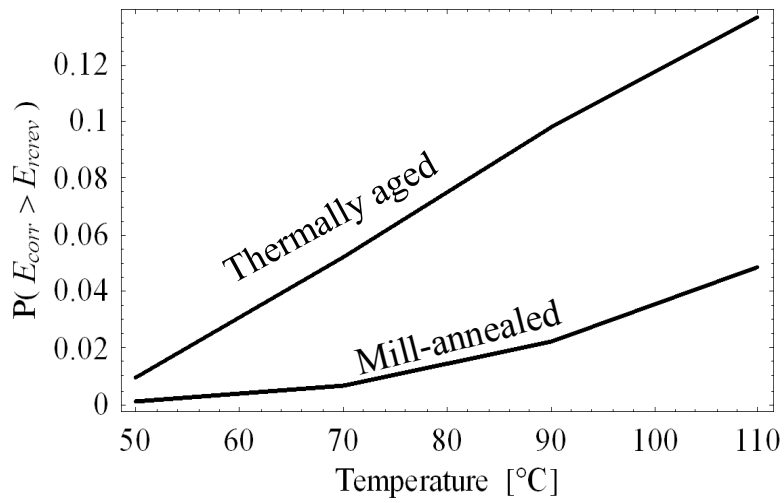
Figure 4

(E)
Figure 4 (Continued)
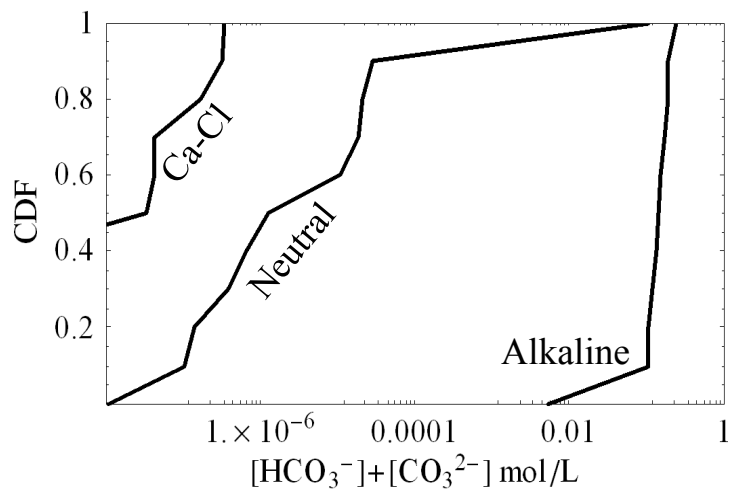
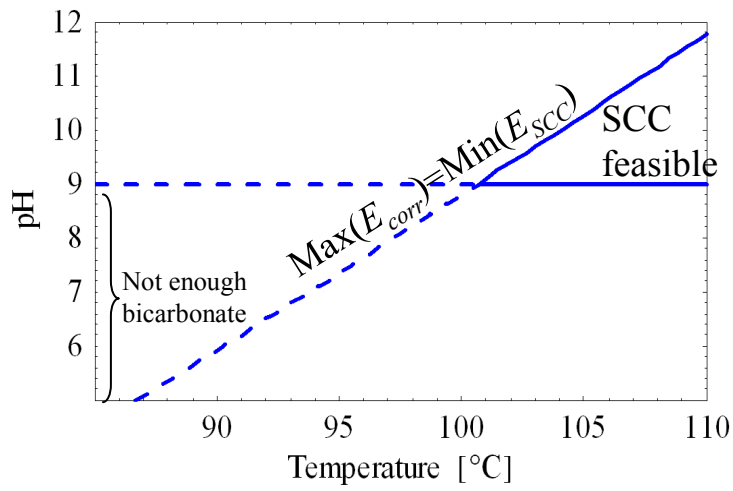Figure 4

.
Figure 5

Figure 6

Figure 7

Figure Captions

Figure 1: Comparison of the corrosion potential computed with Eq. (1) to experimental data published in Reference [3].

Figure 2: Uncertainty in the water vapor content in air near the waste package, as a function of temperature.

Figure 3: Cumulative distribution functions (CDF) of chemical components computed from thermodynamic simulation of evaporation and the chemical divide concept.

Figure 4: Scatter plots of the difference $E_{corr} - E_{rcrev}$ versus various chemical components after evaporation of underground waters. The temperature is 110 °C [230 °F], equations for mill-annealed Alloy 22 were used, and the Monte Carlo mathematical sample included 10^4 points.

Figure 5: Fraction of points satisfying $E_{corr} > E_{rcrev}$ as a function of temperature and Alloy 22 metallurgical state.

Figure 6: Cumulative distribution function (CDF) of total carbonate concentration resulting after evaporation at 110°C [230°F] for the three brine types.

Figure 7: Temperature-pH feasibility region for stress corrosion cracking.